

1



2

3

4

5

6 **Supplementary Information for**

7 Strigolactones promote flowering by inducing the miR319-*LA-SFT*
8 module in tomato

9

10 Ivan Visentin, Leticia Frizzo Ferigolo, Giulia Russo, Paolo Korwin Krukowski, Caterina
11 Capezzali, Danuše Tarkowská, Francesco Gresta, Eleonora Deva, Fabio Tebaldi Silveira
12 Nogueira, Andrea Schubert, Francesca Cardinale*

13

14 *Francesca Cardinale, DISAFA PlantStressLab, largo P. Braccini 2, Grugliasco (TO), 10095
15 Italy. Phone number: +390116708875

16 **Email:** francesca.cardinale@unito.it

17

18 **This PDF file includes:**

19 Supplementary text

20 Figures S1 to S10

21 Tables S1 to S5

22 Legends for Datasets S1 to S3

23 SI References

24 **Other supplementary materials for this manuscript include the following:**

25 Datasets S1 to S3

26 **Supplementary text**

27

28 **Results**

29

30 **Strigolactone deficiency widely affects the transcription of genes in the flowering** 31 **network**

32 Besides the genes highlighted in the manuscript body, we found a down-regulation of several
33 MADS-box transcription factors involved in tomato floral transition (Table S1, Dataset S2),
34 namely the *FRUITFULL-like* genes *FUL1* and *FUL2* (1), *MADS-BOX PROTEIN13* (*MBP13*),
35 *MBP14*, *MBP15*, *MBP18/FYFL*, *MBP20* and *MBP56* (2), *JOINTLESS* (*J*) (3), tomato B-class
36 MADS-box gene *TM6/TDR6* and *AGAMOUS1* (*TAG1*) (4, 5). Three members of the
37 *CONSTANS* (*CO*)/*CONSTANS-like* (*COL*) gene family, related to photoperiodic signaling and
38 flowering in tomato (3), were found down-regulated (*CO1*, *CO3* and *COL4a*), while *COL* was
39 slightly up-regulated. The transcription factor-encoding gene *NAP2* (*NUCLEOSOME*
40 *ASSEMBLY PROTEIN2*) of the NAC (*NAM*, *No apical meristem*; *ATAF*; *CUC*, *Cup-shaped*
41 *Cotyledon*) family, activated by *Apetala3/Pistillata* (*AP3/PI*), is strongly down-regulated (\log_2FC
42 = -4.5). This protein controls both leaf senescence and fruit yield in tomato, and *NAP2*-
43 overexpressing plants start producing flowers around one week earlier than wt plants (6, 7).
44 Three other genes encoding NAC-domain transcription factors, *NAM2* and *NAM3*, and the *NAM*
45 homologue *GOBLET* (*GOB*), involved in floral morphogenesis in tomato (7, 8), were also down-
46 regulated in SL- plants. Other DEGs listed in Table S1 have not been functionally characterized
47 in tomato yet, and have been mainly identified through bioinformatic (9) or transcriptome studies
48 (10, 11) based on the role of their putative homologues in floral transition pathways of *A.*
49 *thaliana* and other model plants. Among down-regulated genes we found the tomato
50 orthologues of the genes coding for: MYB-related transcription factors *LATE ELONGATED*
51 *HYPOCOTYL* (*LHY*) and *CIRCADIAN CLOCK ASSOCIATED 1* (*CCA1*) (12); *TIMING OF CAB*
52 *EXPRESSION 1* (*TOC1*), a member of the *PSEUDO-RESPONSE REGULATOR* (*PRR*) family
53 (9) that controls photoperiodic flowering response in *A. thaliana*, positively regulating *CCA1* and
54 *LHY* expression (13); the *Transducin/WD40 repeat-like superfamily protein* *COP1*, an E3
55 ubiquitin-protein ligase that acts as a repressor of photomorphogenesis and is involved in the
56 degradation of *CO* during the night (14, 15); the *EARLY FLOWERING* (*ELF*) 3 and *ELF4*, which
57 function as modulators of light signal transduction downstream of phytochromes and control
58 photoperiodic flowering by interacting with *COP1* and regulating *GIGANTEA* (*GI*) stability (16,
59 17); and *ELF7*, a RNA polymerase II-associated factor *Paf1* involved in the regulation of
60 flowering time (18). On the other hand, among the most interesting up-regulated genes, we
61 found the one encoding the circadian oscillator *GI*, involved in photoperiod-dependent floral
62 transition in several plant species (19); and a putative orthologue of the AP2-like transcription
63 factor-encoding *TARGET OF EAT1* (*TOE1*) named *AP2d* (20). Moreover, a set of genes
64 encoding transcription factors belonging to the large Nuclear Factor Y (*NF-Y*) family, involved
65 in flowering control (21), were found to be down-regulated in the SL- genotype.

66 Several genes in Table S1 are also related to DNA modifications and chromatin remodeling:
67 the gene coding for the replication protein *RPA1b* is up-regulated (22, 23), while one for the
68 *MULTICOPY SUPPRESSOR OF IRA1* (*MSI1*)-like chromatin-adaptor protein *MSI1* (21) is down-
69 regulated. Also, two genes encoding the DNA mismatch repair proteins *MutS HOMOLOGS*,
70 *MSH1* (24), and *MSH2* (25), are up- and down-regulated, respectively. Three more
71 uncharacterized gene products were identified in the GO enrichments process, all of which
72 were found to be down-regulated in the SL- plants: the putative orthologue of the *A. thaliana*
73 *BONSAI* (*BNS*), encoding an ubiquitin-protein ligase complex that regulates cell cycle
74 progression (26); one encoding the cell wall-localized class III peroxidase *PER17*, the
75 orthologue of which is involved in the transition to flowering and timing of lignified tissue
76 formation in *A. thaliana* (27); and the one encoding a *Snf1*-related kinase-interacting protein
77 (*SKI2*, similar to At1g80940), which is annotated as involved in the regulation of flower
78 development based on InterPro classification.

79

80

81 **Materials and Methods**

82

83 **Plant materials and growth conditions**

84 The tomato *SICCD7*-silenced line 6936, here called SL-, and its wt genotype M82 were a kind
85 gift by Dr. H. J. Klee (University of Florida) (28) and show 70-80% reduction of strigolactone

86 content in root tissues and exudates. The $LA_{pro}>>LA^m-GFP$ genotype (29) expresses *La-2*, a
87 miR319-insensitive version of *LA* (30), under the control of the *LA* promoter and in translational
88 fusion with GFP in the M82 background. Seeds were sterilized in 4% (v/v) sodium hypochlorite
89 containing 0.02% (v/v) Tween 20, rinsed thoroughly with sterile water, and then placed for 48
90 h on moistened filter paper at 25°C in darkness. Plants were grown for two weeks in a walk-in
91 climate chamber (16/8h light/dark 25°C) in a seedbed with standard soil (Terra Nature, NPK
92 12:14:24) and subsequently moved into 5-liter pots under greenhouse conditions. From the
93 transplanting to the end of the experiments, plants were fertilized with a standard half-strength
94 Hoagland solution twice a week. Plant age was counted starting at the emergence of cotyledons
95 from the soil bed.

96 For the experiment described in fig. 2A and S3A, 4-day-old M82 wt plants were sprayed until
97 runoff on the whole aerial part with a 5 μ M solution of GR24^{5DS} (synthetic strigolactone analogue
98 from StrigoLab Srl, Turin, Italy) in 0.01% v/v acetone in water (n=6-13). Analogously, the control
99 plants were sprayed with a corresponding acetone solution. Six days after the first treatment,
100 when around 50% of the plants were at the transition stage, the plants were split in two groups:
101 group 1 was not further treated (fig. S3A) while group 2 received an additional GR24^{5DS}
102 treatment (fig. 2A). The meristems were evaluated 4 to 12 days after the first treatment under
103 the stereomicroscope and classified as vegetative meristem (VM), transition meristem (TM),
104 inflorescence meristem (IM) or floral meristem (FM).

105 For the leaf-spraying experiment described in fig. 2B-E, 3-week-old wt plants grown under the
106 same conditions mentioned above were sprayed with the same 5 μ M solution of GR24^{5DS} in
107 0.01% v/v acetone in water, or with a corresponding acetone solution (n=8). Ripening fruits (31)
108 were counted until 80 days, and weighed until 92 days after the treatment. Leaves (about 100
109 mg fw) were collected as above 2, 6, and 24 hours after the treatment and stored at -80°C until
110 analysis. For the leaf-spraying experiments described in fig. 3C-E, 8-day-old or 4-week-old wt
111 and $LA_{pro}>>LA^m-GFP$ plants were treated as above with GR24^{5DS} (n=8). The number of leaves
112 to the first inflorescence was counted at anthesis (*i.e.* stage 3 as defined earlier (32)). For the
113 experiment in fig. 3A, 4-week-old wt plants were grown and treated as in the experiment in fig.
114 2B-E (n=5). For each plant, a sample consisting of three young leaves was collected 0, 15', 1h,
115 6h and 24h after treatment. The samples were processed for gene transcript quantification as
116 described below. For the experiment in fig. 4 and S5, vegetative wt plants were treated with 5
117 μ M GR24^{5DS} 8 days after seedling emergence, and harvested one week later; another subset
118 was treated in the reproductive phase, 23 days after germination, and harvested at 30 days.
119 Each treatment had n=6 (each sample the pool of 10 individual meristems).

120 For the grafting experiment described in fig. 1, 3B, S2A-B, three grafted lines were produced
121 by the clamp-grafting technique on plants at the 2/4-leaf stage (about 3 weeks after seedling
122 emergence) and with a stem diameter of 1.5–2 mm (n=5; wt or SL- rootstock and scion, wt/wt
123 or SL-/SL-, respectively; and wt scion grafted to a SL- rootstock, wt/SL-). After 3 additional
124 weeks of acclimation, grafted plants were transplanted and grown in the greenhouse as above.
125 The daily count of new individual flowers at anthesis started 3 weeks after graft production (*i.e.*
126 at transplant) and continued for 3 weeks. A subset of self-grafted wt/wt plants were treated 1
127 and 3 weeks after grafting with 5 μ M GR24^{5DS}. Ripening fruits (31) were counted and weighed
128 60 days after grafting. For gene transcript quantification, leaves of comparable physiological
129 stage (about 100 mg fw) were collected 20 days after grafting from each plant, deep-frozen,
130 and stored at -80°C until analysis.

131 For transcriptome analysis, at least 3 fully expanded leaves were collected (one per plant) from
132 5 wt and SL- plants, grown for 3 weeks after seedling emergence in a walk-in climate chamber
133 set at 16/8h light/dark 25°C. Leaves were collected at 9.00 am, 3 h into the light period.

135 **Library construction, sequencing, and processing of mRNA data**

136 Total RNA was extracted from 3-week-old wt and SL- tomato leaves using the Spectrum Plant
137 Total RNA Kit (Sigma Aldrich). After digestion of contaminant DNA by DNase I
138 (ThermoScientific) at 37°C for 30 min, RNA quantity and quality were determined with a
139 Nanodrop 2000 spectrophotometer (Thermo Fisher Scientific Inc., Wilmington, DE, United
140 States) and sent to Novogene Europe for library construction and sequencing (Cambridge,
141 United Kingdom). There, RNA degradation and contamination were monitored on 1% agarose
142 gels, RNA purity was checked using the NanoPhotometer® spectrophotometer (IMPLEN, CA,
143 USA), and RNA integrity (RIN>6) and quantities were assessed using the RNA Nano 6000
144 Assay Kit of the Bioanalyzer 2100 system (Agilent Technologies, CA, USA). cDNA libraries
145 were prepared from 1 μ g total RNA using NEBnext Ultra TM RNA Library Prep Kit for Illumina

146 (NEB, USA) following the manufacturer's recommendations. A total of six libraries (three each
147 for wt and SL- leaves) were constructed and quantified using a Qubit 2.9 fluorometer (Life
148 Technologies) and sequenced on an Illumina platform to generate paired-end reads. Raw reads
149 of FASTQ format were processed through in-house scripts and clean reads were obtained by
150 removing reads containing adapter, poly-N sequences and reads with low quality. A total of
151 35825 high-quality, clean reads were mapped using HISAT2 (33) to the reference genome of
152 *Solanum lycopersicum* cv "Heinz 170" assembly ITAG SL3.0
153 (https://www.ebi.ac.uk/ena/data/view/GCA_000188115.3). Expressed genes passing quality
154 checks, trimming and FPKM filtering are listed in Table S4. The number of mapped reads for
155 each gene was counted using htseq-count (34). Values of fragments per kilobase of exon per
156 million fragments mapped (FPKM) for the assembled transcription units were calculated. After
157 filtering and trimming, approximately 31.63 to 47.29 million clean pair-end reads were obtained
158 from each of the six libraries. Expressed tomato genes ranged from 18261 (sample SL-_2) to
159 19048 (sample wt_3, Table S4), using a cut-off FPKM value > 0.3 to declare a gene as
160 expressed. The DESeq2 R package was used to normalize expression levels and perform
161 differential expression analysis based on the negative binomial distribution (35). Following read
162 count normalization, the resulting P values were adjusted using the Benjamini and Hochberg's
163 approach for controlling the False Discovery Rate (FDR). Genes with a Benjamini–Hochberg
164 adjusted p value/FDR < 0.05 and a log₂ fold change (log₂FC) >+0.7;<-0.7 were assigned as
165 DEGs. A high Pearson's correlation coefficient (r) was observed among FPKM values of
166 biological replicates of the same genotype and condition in the sequenced set (average r =
167 0.92). Considering the mean of three biological replicates for each genotype, 18013 genes were
168 found to be expressed in both lines, while 983 genes were only expressed in wt and 696 genes
169 in SL- plants (fig. S10A). A total of 8166 protein-coding genes were found differentially
170 expressed (DEGs) in the SL- plants with respect to wt (FDR ≤ 0.05; Dataset S3), corresponding
171 to 23.56% of the predicted protein-coding genes. These genes were additionally filtered based
172 on their log₂ FC (thresholds -0.7 > log₂FC > +0.7). After filtering, we obtained a dataset of 7140
173 DEGs, which display a higher proportion of down-regulated genes in the SL- plants (5412) in
174 comparison to up-regulated genes (1728) (fig. S10B). To confirm the RNAseq results, we
175 analyzed the expression of selected genes by qRT-PCR, focusing on flowering-related loci. Fig.
176 S8 shows high correlation between transcript levels observed in the RNAseq dataset and in
177 targeted qRT-PCR on independent samples.

178 179 **Functional analysis of tomato DEGs**

180 Enrichment analysis of each DEG gene ontology (GO) term and KEGG pathway (36) was
181 performed with the ShinyGO v0.61 GO Enrichment Analysis tool using default parameters
182 (<http://bioinformatics.sdstate.edu/go/>) (37) and comparing the frequency of query genes with
183 the complete reference genome for *S. lycopersicum* (SL 3.0). Enrichment analyses were based
184 on a hypergeometric distribution followed by FDR correction. Significant GO terms and KEGG
185 functional categories (FDR < 0.05) were reported.

186 187 **Gibberellin treatments and quantification**

188 For the assessment of general gibberellin sensitivity, 2-week-old wt and SL- plants (n=8) were
189 sprayed on the whole aerial part with a 10 μM solution of GA₃ (Sigma-Aldrich) until runoff.
190 Control plants were sprayed with a corresponding volume of water only. The increment of the
191 first internode length was measured every five days, starting from five days after the treatment
192 and reported as the difference between the measured values of GA₃-treated and mock-treated
193 plants of the same genotype at the same time point.

194 The sample preparation and analysis of gibberellins were performed as described (38) with
195 some modifications. Briefly, tissue samples of about 5 mg dry weight (DW) from n=3 biological
196 replicates were ground to a fine powder using 2.7-mm zirconium oxide beads (Retsch GmbH
197 & Co. KG, Haan, Germany) and a MM 400 vibration mill at a frequency of 30 Hz for 3 min
198 (Retsch GmbH & Co. KG, Haan, Germany) with 1 mL of ice-cold 80 % acetonitrile
199 containing 5 % formic acid as extraction solution. The samples were then extracted overnight
200 at 4 °C using a benchtop laboratory rotator Stuart SB3 (Bibby Scientific Ltd., Staffordshire, UK)
201 after adding 17 internal gibberellin standards ([²H₂]GA₁, [²H₂]GA₃, [²H₂]GA₄, [²H₂]GA₅, [²H₂]GA₆,
202 [²H₂]GA₇, [²H₂]GA₈, [²H₂]GA₉, [²H₂]GA₁₅, [²H₂]GA₁₉, [²H₂]GA₂₀, [²H₂]GA₂₄, [²H₂]GA₂₉, [²H₂]GA₃₄,
203 [²H₂]GA₄₄, [²H₂]GA₅₁, and [²H₂]GA₅₃ (OChemIm, Czech Republic). The homogenates were
204 centrifuged at 36,670 g and 4 °C for 10 min, then the corresponding supernatants were further
205 purified using mixed-mode SPE cartridges (Waters, Milford, MA, USA) and analyzed by ultra-

206 high performance liquid chromatography-tandem mass spectrometry (UHPLC-MS/MS;
207 Micromass, Manchester, UK). Gibberellins were detected using multiple-reaction monitoring
208 mode of the transition of the ion $[M-H]^-$ to the appropriate product ion. The Masslynx 4.2
209 software (Waters, Milford, MA, USA) was used to analyze the data and the standard isotope
210 dilution method (39) was used to quantify endogenous gibberellin levels.

211

212 **Gene transcript quantification**

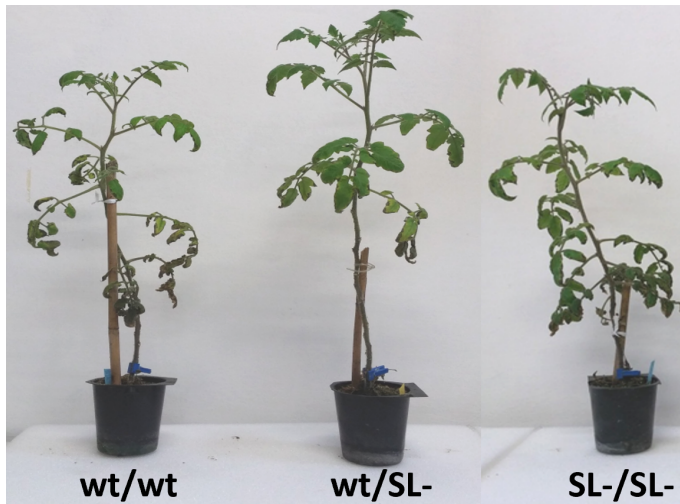
213 Total RNA from tomato leaves was extracted with the Spectrum Plant Total RNA Kit (Sigma
214 Aldrich) and treated with DNase I (ThermoScientific) at 37°C for 30 min to remove residual
215 genomic DNA. First-strand cDNA was synthesized from 3 µg of purified total RNA using the
216 High-Capacity cDNA Reverse Transcription Kit (Applied Biosystems) according to the
217 manufacturer's instructions. A modified protocol with a stem-loop primer (40) was followed for
218 targeted miR319 and miR156 cDNA synthesis. qRT-PCR was carried out in a StepOnePlus
219 machine (Applied Biosystems) using the SYBR method (Luna Universal One-Step RT-qPCR
220 Kit, New England Biolabs); for loci and primers, see Table S4. Transcript concentrations were
221 normalized on *ACTIN (ACT)*, *ELONGATION FACTOR-1α (EF-1α)* or *small nuclear RNA U6*
222 (*snU6*) transcripts as endogenous controls. Three independent biological replicates were
223 analyzed as a minimum, and each qRT-PCR reaction was run in technical triplicates. Transcript
224 amounts were quantified through the $2^{-\Delta\Delta C_t}$ method.

225

226 **Statistical analysis**

227 Significant differences among grafted plants were statistically analyzed by applying a one-way
228 ANOVA test and Tukey's HSD post-hoc test was used for mean separation when ANOVA
229 results were significant ($p < 0.05$). Significant differences of pairwise comparisons were
230 assessed by Student's t test. The SPSS statistical software package (SPSS Inc., Cary, NC,
231 v.22) was used. RNAseq results were validated via qRT-PCR as previously done (41) on genes
232 related to flowering. In short, \log_2FC values of *SFT* (Soly03g063100.2), *SP5G*
233 (Soly05g053850.3), *SP6A* (Soly05g055660.2), *MBP20* (Soly02g089210.3), *FUL1*
234 (Soly06g069430.3), *LA* (Soly07g062680.2), *GA2ox4* (Soly07g061720.3), *GA2ox2*
235 (Soly06g035530.3), *GA3ox2* (Soly03g119910.3) were obtained from both RNAseq and qRT-
236 PCR analyses by contrasting SL- with wt plants. The Spearman's rank correlation method (42)
237 was used to analyze the correlation between these two datasets. A Spearman's $\rho \geq 0.75$ was
238 used as threshold to consider two datasets positively highly correlated.

239 **A**



240

241

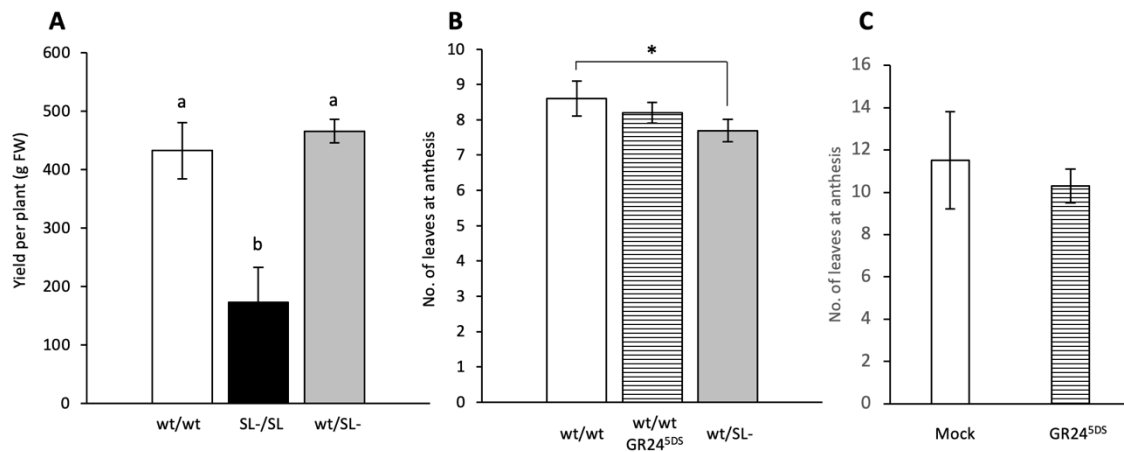
242 **B**



243

244

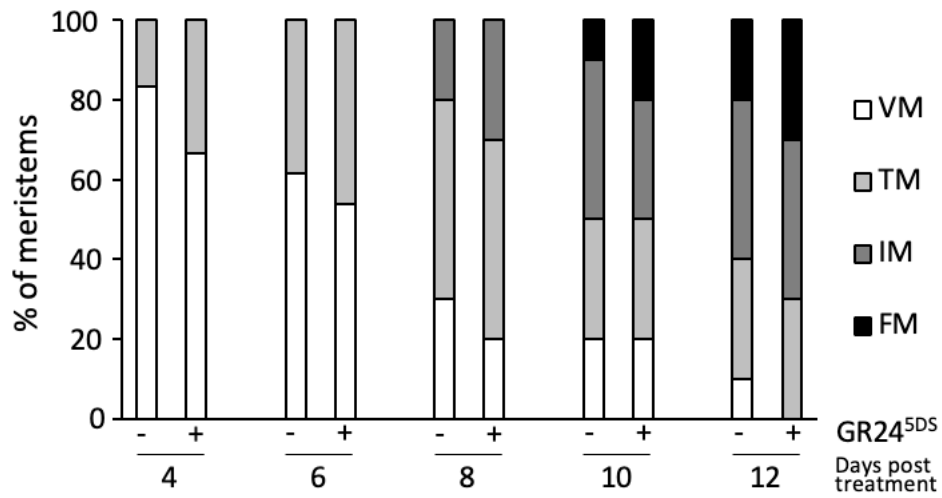
245 **Fig. S1. (A)** Appearance of wt/wt, wt/SL- and SL-/SL- plants 30 days after grafting. **(B)** Tomato
246 plants cv M82 at anthesis (around 5 weeks from seedling emergence). The plant on the right
247 was treated with 5 μ M GR24^{5DS} 8 days after seedling emergence, while the plant on the left
248 was mock treated at the same age.



250
 251
 252
 253
 254
 255
 256
 257
 258
 259
 260
 261

Fig. S2. Effects of different grafting combinations and/or treatment with 5 μM GR24^{5DS} on (A) cumulative yield per plant in homo- or hetero-grafting of wt and strigolactone-depleted (SL-) scions and rootstocks. (B) Comparisons between the number of leaves at the time of anthesis in mock-treated wt/wt plants, wt/SL- plants and wt/wt plants or (C) non-grafted wt plants treated with 5 μM GR24^{5DS} (1 and 3 weeks after grafting). Data represent the mean ± SE of n=10 biological replicates. * indicates significant differences between wt/wt plants and wt/SL- plants, as determined by Student's t test ($p < 0.05$). In panel A the letters indicate significant differences as determined by a one-way ANOVA test and Tukey's HSD post-hoc test ($p < 0.05$).

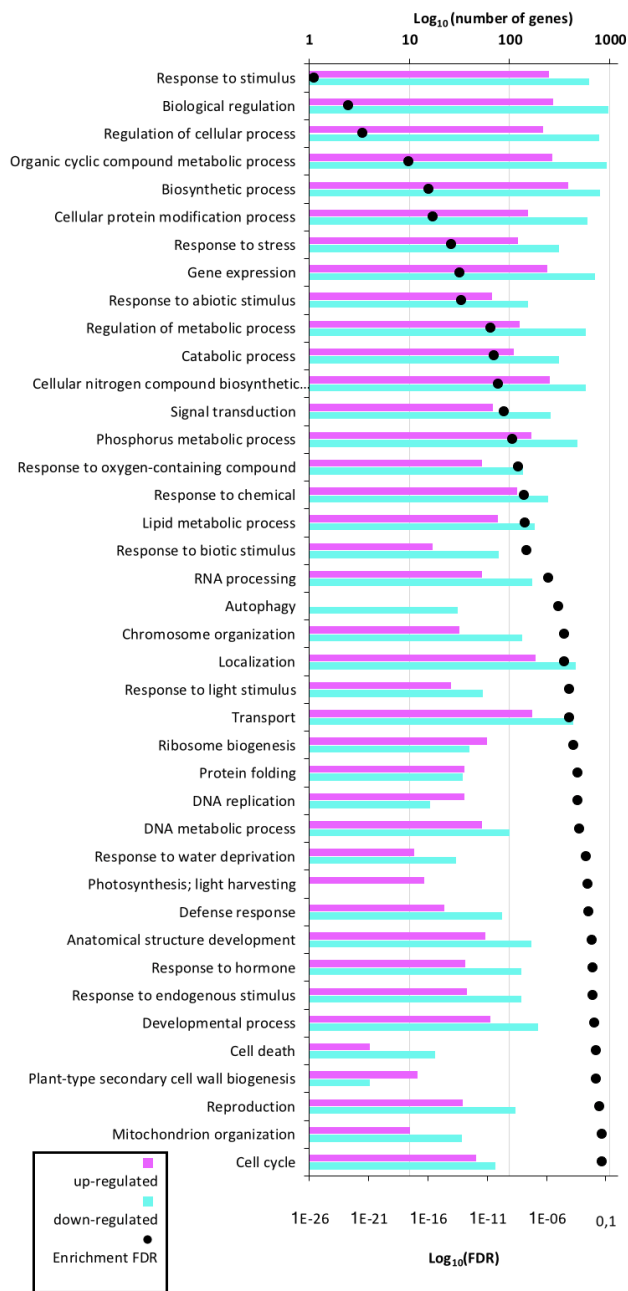
262



263

264

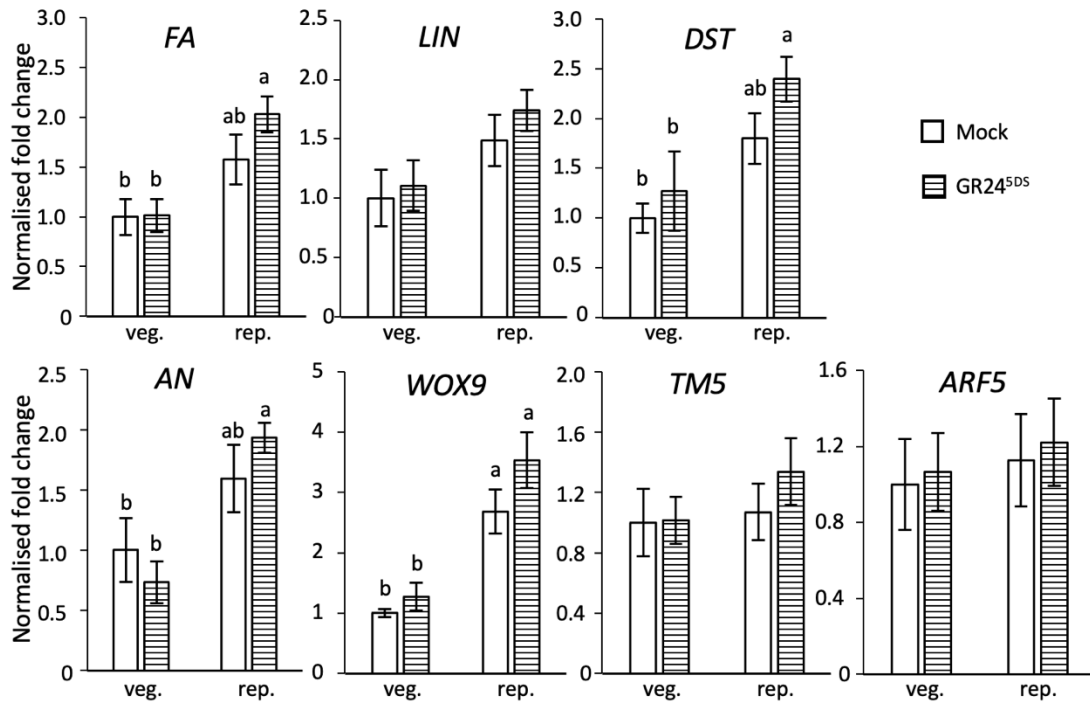
265 **Fig. S3.** Meristem maturation of mock- or GR24^{5DS}-treated plants. For representative images
266 of the four sequential developmental stages: vegetative meristem (VM), transition meristem
267 (TM), inflorescence meristem (IM) and floral meristem (FM), see fig. 2A. Plants were treated
268 with a 5 μ M solution 4 days after seedling emergence, i.e. before floral transition. The
269 meristems were evaluated under the stereomicroscope 4 to 12 days after the treatment (n=6-
270 13).



272

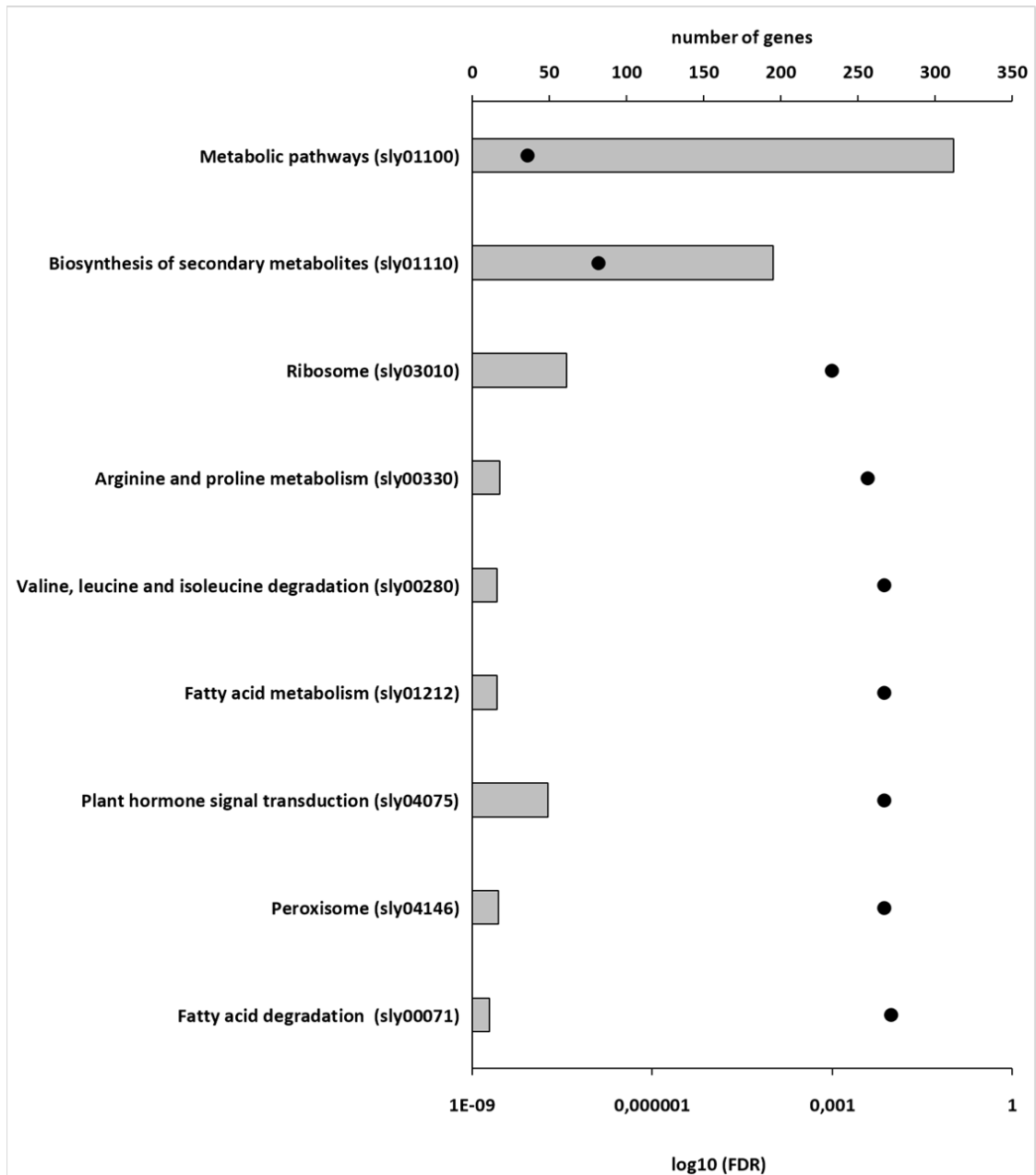
273

274 **Fig. S4.** Functional GO categories from the BP-GO enrichment of DEGs in strigolactone-
 275 depleted leaves in comparison to wt. Light blue and fuchsia bars indicate the number of up-
 276 and down-regulated DEGs, respectively. Black dots show the Log₁₀FDR value of each enriched
 277 category, with FDR < 0.05 as a threshold.



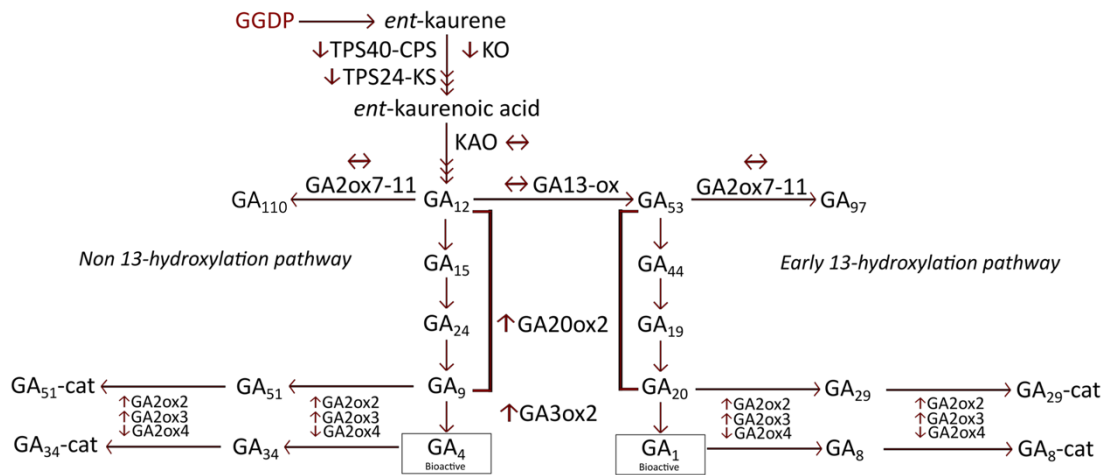
278

279 **Fig. S5.** Effects of exogenous strigolactones and age on the transcripts of marker genes for
 280 meristematic development: *FA* (*FALSIFLORA*); *LIN* (*LONG INFLORESCENCE*); *DST*
 281 (*DELAYED SYMPODIAL TERMINATION*); *AN* (*ANANTHA*); *WOX9* (*WUSCHEL-RELATED*
 282 *HOMEBOX9*); *TM5* (*TOMATO MAD5*); *ARF5* (*AUXIN RESPONSE FACTOR5*). Vegetative
 283 (veg.) wt plants were treated with 5 μ M GR24^{5DS} 8 days after seedling emergence, and
 284 harvested one week later; another subset was treated in the reproductive (rep.) phase, 23 days
 285 after germination, and harvested 30 days after germination. Transcript abundances were
 286 normalized to endogenous *EF1 α* and *ACT* and presented as fold-change value over mean
 287 values of meristems in untreated vegetative plants, which were set to 1. Data represent the
 288 mean \pm SE of n=6 biological replicates (each the pool of 10 apical meristems) analyzed in
 289 technical triplicates. Different letters on top of bars indicate statistically significant differences
 290 among all samples as determined with one-way ANOVA followed by Tukey's post-hoc test; no
 291 significant differences for pairwise comparisons between treated and untreated samples of the
 292 same age could be detected by Student's t-test ($p < 0.05$).



293
 294
 295
 296
 297
 298

Fig. S6. KEGG pathways categories enriched among DEGs in leaves of strigolactone-depleted tomato plants in comparison to wt. Grey bars indicate the number of DEGs and black dots show the Log₁₀FDR value for each enriched KEGG pathway category identified by the KEGG ID in brackets, with FDR < 0.05 as a threshold.



299

300

301

302

303

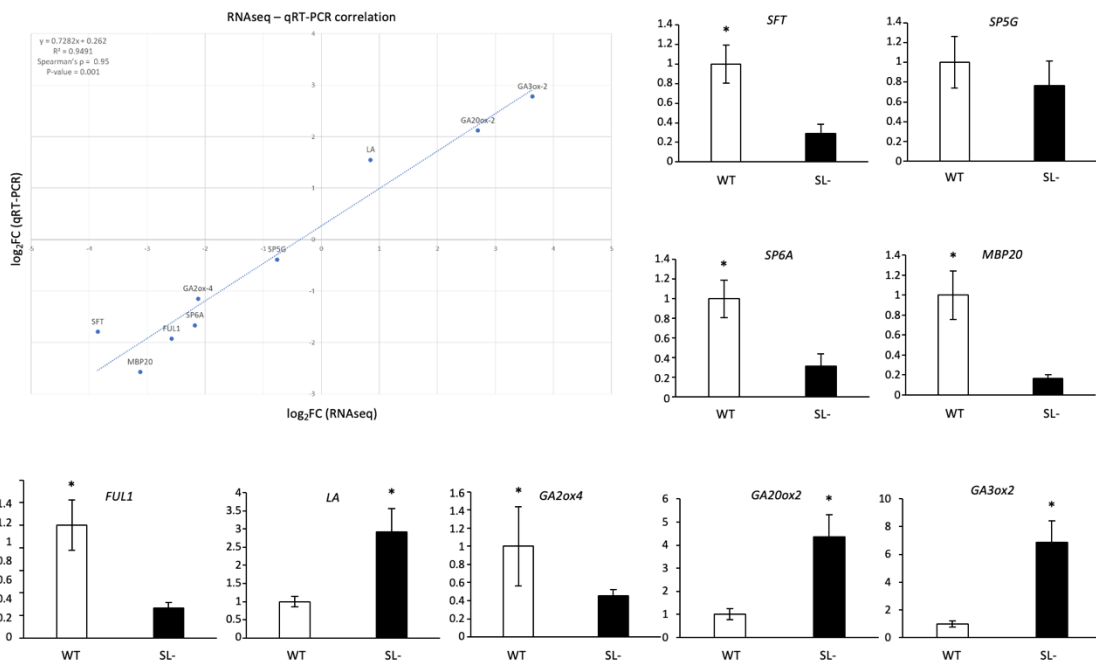
304

305

306

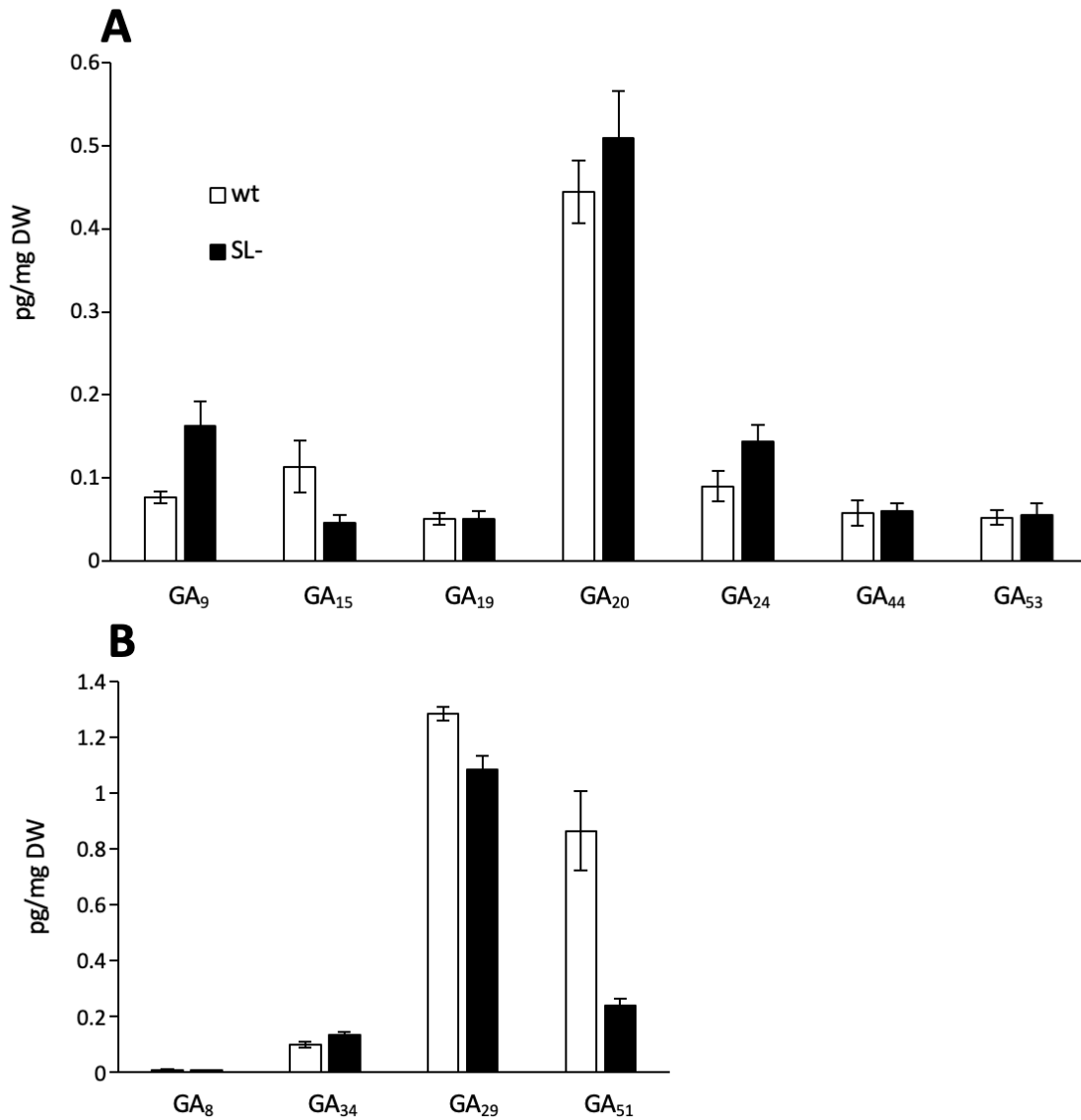
307

Fig. S7. Schematic representation of the tomato gibberellin (GA) biosynthetic pathway. GGDP, geranylgeranyl diphosphate; CPS (TPS40), *ent*-copalyl diphosphate synthase; KS (TPS24), *ent*-kaurene synthase; KO, *ent*-kaurene oxidase; KAO, *ent*-kaurenoic acid oxidase; GA13ox, GA 13-oxidase; GA20ox, GA 20-oxidase; GA3ox, GA 3-oxidase; GA2ox, GA 2-oxidase; GA-cat, GA-catabolite. Arrows by gene acronyms indicate whether each gene is up- or down-regulated, or remains stable in strigolactone-depleted plants compared to the wt.



309

310 **Fig. S8.** RNAseq validation through qRT-PCR analysis. **Upper left:** correlation between
 311 RNAseq (x-axis) and qRT-PCR (y-axis) \log_2FC values of transcripts obtained by comparing
 312 strigolactone-depleted (SL-) and wt plants. Correlation was calculated through the Spearman's
 313 rank correlation method (Spearman's ρ and p-value, R^2 and best-fit line equation are shown).
 314 **All other panels:** validation of the RNAseq analysis by qRT-PCR. Transcript quantification of
 315 *SFT* (Solyc03g063100.2); *SP5G* (Solyc05g053850.3); *SP6A* (Solyc05g055660.2); *MBP20*
 316 (Solyc02g089210.3); *FUL1* (Solyc06g069430.3); *LA* (Solyc07g062680.2); *GA2ox4*
 317 (Solyc07g061720.3); *GA2ox2* (Solyc06g035530.3); *GA3ox2* (Solyc03g119910.3). Transcript
 318 abundances were normalized to endogenous *EF1 α* and *ACT* and presented as fold-change
 319 values over mean values of wt plants, which were set to 1. Data represent the mean \pm SE of
 320 $n=3$ biological replicates. * indicates significant differences as determined by Student's t test (p
 321 < 0.05).



322
323
324
325
326
327
328

Fig. S9. Effect of strigolactone deprivation on gibberellin metabolism. **(A)** Concentration of the biosynthetic precursors of bioactive gibberellins and **(B)** of their deactivation products in wt and strigolactone-depleted (SL-) plants. Data represent the mean \pm SE of n=3 biological replicates analyzed in technical quadruplicates. See fig. S7 for metabolite positioning in the gibberellin pathway.

329

330

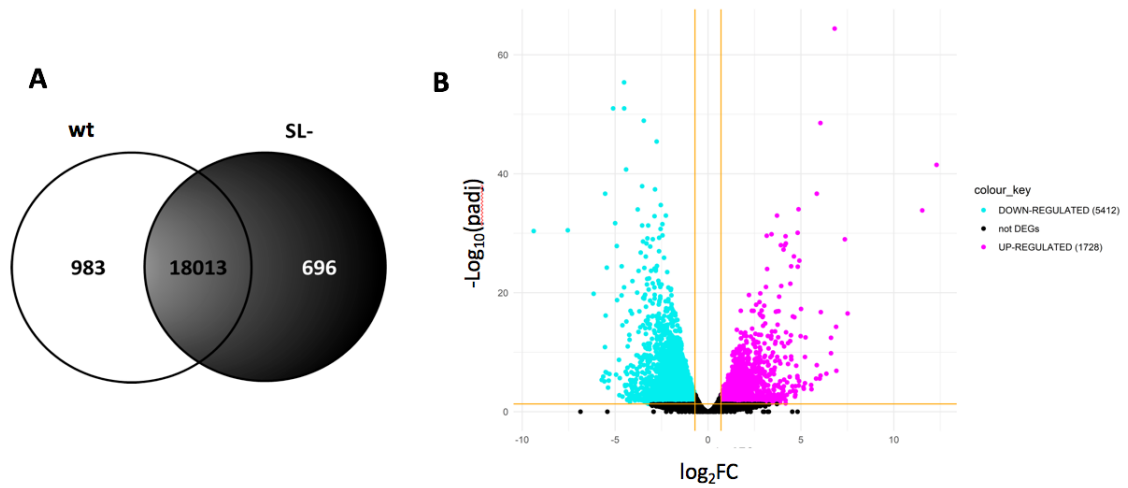
331

332

333

334

335



336

337

338

339 **Fig. S10.** Comparison of expressed genes between wt and strigolactone-depleted (SL-) tomato
340 lines. **(A)** Venn diagram displaying the number of genes identified in either or both genotypes;
341 **(B)** volcano plot of the number and distribution of up- and down-regulated DEGs (FDR < 0.05,
342 log₂FC >+0.7 and <-0.7 respectively), showing statistical significance (padjust) versus
343 magnitude of change (fold change, FC).

344
345
346

Table S1. Selection of tomato DEGs between wt and strigolactone-depleted leaves related to flowering and/or included in the GO category Reproduction (GO: 0000003). A comprehensive list of all DEGs related to this category can be found in Dataset S2.

Gene ID	log ₂ FC	ITAG3.0 annotation	<i>S. lycopersicum</i> gene acronym	<i>A. thaliana</i> orthologue	<i>A. thaliana</i> acronym
Solyc03g119910.3	3.64	<i>Le3OH-23b-hydroxylase</i>	GA3ox2	AT1G15550	GA3OX1
Solyc04g054150.1	2.84	<i>Nuclear transcription factor Y protein</i>	NF-YB3	AT4G14540	NF-YB3
Solyc06g035530.3	2.70	<i>Gibberellin 20-oxidase-2</i>	GA20ox2	AT5G51810	GA20OX2
Solyc08g005610.3	2.29	<i>Abscisic acid 8'-hydroxylase</i>	CYP707A2	AT5G45340	CYP707A3
Solyc04g071990.3	2.15	GIGANTEA	GI	AT1G22770	GI
Solyc06g069230.3	1.98	<i>DNA mismatch repair protein</i>	MSH2	AT3G18524	MSH2
Solyc03g093610.1	1.67	<i>Ethylene response factor A.2</i>	ERFA2	AT5G47220	ERF2
Solyc03g115050.3	1.63	<i>Replication A 70 kDa DNA-binding subunit</i>	RPA1B	AT5G08020	RPA1B
Solyc11g072600.2	1.14	APETALA 2d	AP2d	AT2G28550	TOE1
Solyc07g006630.3	0.97	CONSTANS-like protein	COL	AT5G15850	CO
Solyc07g062680.2	0.85	Lanceolate	LA	AT3G15030	TCP4
Solyc02g084630.3	-0.72	<i>TDR6 transcription factor</i>	TM6/TDR6	AT5G23260	AGL32/TT16
Solyc05g053850.3	-0.76	SELF PRUNING 5G	SP5G	AT1G65480	FT
Solyc11g010570.2	-0.78	Jointless	J	AT2G22540	AGL22/SVP
Solyc12g056460.2	-1.07	<i>MADS box transcription factor</i>	MBP14	AT2G45660	AGL20
Solyc12g096500.2	-1.08	CONSTANS-like protein	COL4a	AT5G24930	COL4
Solyc03g121010.3	-1.21	<i>RNA polymerase II-associated factor 1 like</i>	ELF7	AT1G79730	ELF7
Solyc01g079870.3	-1.21	CONSTANS interacting protein 2b	NF-YC9	AT1G08970	NF-YC9
Solyc10g009080.3	-1.36	<i>Squamosa promoter binding protein 3</i>	SBP3	AT2G33810	SPL3
Solyc11g011980.2	-1.37	<i>Transducin/WD40 repeat-like superfamily protein</i>	COP1	AT2G32950	COP1
Solyc02g089540.3	-1.40	CONSTANS 1	CO1	At5G15841	CO
Solyc03g006830.3	-1.46	<i>MADS-box transcription factor</i>	MBP18/FYFL	AT5G62165	AGL42
Solyc01g098390.3	-1.52	<i>Gibberellin receptor</i>	GID1a	AT3G05120	GID1A
Solyc03g117670.3	-1.55	<i>Snf1-related kinase interacting protein</i>	SKI2	AT1G80940	-
Solyc09g074270.3	-1.57	<i>Gid1-like gibberellin receptor</i>	GID1b1	AT3G63010	GID1B
Solyc01g008490.3	-1.61	<i>Nuclear transcription factor Y subunit</i>	NF-YA1	AT5G12840	NF-YA1

Solyc10g005080.3	-1.64	Late elongated hypocotyl and circadian clock associated-1-like protein 1	LHY	AT1G01060	LHY
Solyc08g065870.3	-1.69	EARLY FLOWERING 3	ELF3	AT2G25930	ELF3
Solyc08g006570.3	-1.70	ANAPHASE-PROMOTING COMPLEX 13 Bonsai protein	Solyc08g006570	AT1G73177	APC13/BNS
Solyc11g010120.2	-1.72	Peroxidase	PER17	AT2G22420	PRX17
Solyc02g084740.3	-1.87	Cytochrome P-50 - 3-epi-6-deoxocathasterone 23-monooxygenase	CYP90C2/DUMPY	AT4G36380	ROT3
Solyc01g087240.3	-1.96	Nuclear transcription factor Y subunit A-9	NF-YA9	AT3G20910	NF-YA9
Solyc07g061720.3	-2.12	Gibberellin 2-oxidase 4	GA2ox4	AT1G78440	GA2OX1
Solyc08g062210.3	-2.13	Nuclear transcription factor Y subunit	NF-YA8	AT1G17590	NF-YA8
Solyc08g080100.3	-2.17	MADS-box transcription factor	MBP13	AT4G22950	AGL19
Solyc05g055660.2	-2.18	Flowering locus T protein	SP6A	AT1G65480	FT
Solyc07g049530.3	-2.22	1-Aminocyclopropane-1-carboxylate oxidase 1	ACO1	AT2G19590	ACO1
Solyc07g062840.3	-2.25	Goblet	GOBLET	AT5G53950	CUC2
Solyc03g115770.2	-2.40	Timing of cab expression 1/pseudo-response regulator 1	TOC1	AT5G61380	TOC1
Solyc09g090890.2	-2.41	DNA mismatch repair protein	MSH1	AT3G24320	MSH1
Solyc06g069710.3	-2.42	NAC domain protein	NAM3	AT5G61430	NAC100
Solyc03g115850.3	-2.52	NAC domain-containing protein	NAM2	AT5G61430	NAC100
Solyc06g069430.3	-2.58	FRUITFULL-like MADS-box 1	FUL1	AT3G30260	AGL79
Solyc01g006930.3	-2.88	Nuclear transcription factor Y subunit A-10, putative	NF-YA10	AT5G06510	NF-YA10
Solyc12g087830.2	-2.98	MADS-box transcription factor	MBP15	AT1G47760	AGL102
Solyc11g020290.2	-3.07	WD-40 repeat-containing protein MSI1	WDR238	AT5G58230	MSI1
Solyc02g089210.3	-3.12	MADS box transcription factor	MBP20	AT1G69120	AP1
Solyc02g089520.2	-3.46	CONSTANS protein	CO3	At5G15840	CO

Solyc12g009050.2	-3.46	<i>Nuclear transcription factor Y subunit</i>	<i>NF-YA3</i>	AT1G72830	<i>NF-YA3</i>
Solyc03g063100.2	-3.85	<i>Single flower truss</i>	<i>SP3D; SFT</i>	AT1G65480	<i>FT</i>
Solyc12g042967.1	-3.87	<i>Agamous-like MADS-box protein AGL80</i>	<i>MADS56</i>	AT5G48670	<i>AGL80</i>
Solyc06g051680.1	-4.13	<i>Protein EARLY FLOWERING 4</i>	<i>ELF4</i>	AT2G40080	<i>ELF4</i>
Solyc04g005610.3	-4.51	<i>NAC domain protein NAC2</i>	<i>NAP2</i>	AT1G69490	<i>NAC029</i>
Solyc03g114830.3	-4.75	<i>FRUITFULL-like MADS-box 2</i>	<i>MBP7/FUL/FUL2</i>	AT5G60910	<i>AGL8</i>

347

348

349
350
351

Table S2. Tomato DEGs involved in auxin biosynthesis and metabolism ([GO:0009851] and [GO:0009850]), transport and export ([GO:0009926] and [GO:0010315]), and responses ([GO:0009734] and [GO:0009733]) as retrieved after the differential expression analysis.

Gene ID	log ₂ FC	ITAG 3.0 annotation	<i>S. lycopersicum</i> gene acronym	<i>A. thaliana</i> orthologue	<i>A. thaliana</i> gene acronym
auxin biosynthetic process [GO:0009851], auxin metabolic process [GO:0009850]					
Solyc09g064160.3	3.815015	<i>Flavin-containing monooxygenase</i>	<i>Solyc09g064160</i>	AT4G28720	<i>YUC8</i>
Solyc05g006220.3	-1.77763	<i>IAA-amino acid hydrolase</i>	<i>Solyc05g006220</i>	AT1G51760	<i>IAR3</i>
Solyc05g006220.4	0.844649	<i>IAA-amino acid hydrolase</i>	<i>Solyc05g006220</i>	AT1G51760	<i>IAR3</i>
Solyc05g006220.5	0.988377	<i>IAA-amino acid hydrolase</i>	<i>Solyc05g006220</i>	AT1G51760	<i>IAR3</i>
auxin polar transport [GO:0009926], auxin export across the plasma membrane [GO:0010315]					
Solyc02g089263.1	-0.93593	<i>Auxin transport protein BIG</i>	<i>Solyc02g089263</i>	AT3G02260	<i>TIR3</i>
Solyc05g026140.3	-0.70524	<i>Uncharacterized protein</i>	<i>Solyc05g026140</i>	AT2G31190	<i>RUS2</i>
Solyc01g099120.3	0.65156	<i>Auxin response 4</i>	<i>AXR4</i>	AT1G54990	<i>AXR4</i>
Solyc03g118740.3	0.89916	<i>Auxin efflux facilitator</i>	<i>PIN1</i>	AT1G73590	<i>PIN1</i>
Solyc10g078370.2	-0.90325	<i>Auxin efflux facilitator</i>	<i>PIN9</i>	AT1G73590	<i>PIN1</i>
auxin-activated signaling pathway [GO:0009734], response to auxin [GO:0009733]					
Solyc03g114480.3	-2.84071	<i>Tetraspanin-8</i>	<i>Solyc03g114480</i>	AT4G28050	<i>TET7</i>
Solyc04g076850.3	-1.35286	<i>Entire</i>	<i>E</i>	AT5G65670	<i>IAA9</i>
Solyc11g072480.2	2.37454	<i>Tetraspanin-3</i>	<i>Solyc11g072480</i>	AT3G45600	<i>TET3</i>
Solyc02g082450.3	-1.34272	<i>Auxin efflux facilitator</i>	<i>Solyc02g082450</i>	AT2G17500	<i>PIN-likes5</i>
Solyc02g079190.3	-1.09298	<i>Auxin F-box protein 5</i>	<i>Solyc02g079190</i>	AT3G62980	<i>TIR1</i>
Solyc03g059390.3	-1.42873	<i>Tetraspanin-2</i>	<i>TET2</i>	AT2G19580	<i>TET2</i>
Solyc01g096070.3	-1.18782	<i>Auxin response factor 18</i>	<i>ARF18</i>	AT4G23980	<i>ARF9</i>
Solyc04g049080.3	-1.11164	<i>Tetraspanin-6</i>	<i>Solyc04g049080</i>	AT4G23410	<i>TET5</i>
Solyc02g077560.3	-0.85503	<i>Auxin response factor 3</i>	<i>Solyc04g049080</i>	AT2G33860	<i>ARF3</i>
Solyc12g042075.1	-0.77682	<i>Auxin-response factor</i>	<i>Solyc12g042075</i>	AT5G62000	<i>ARF2</i>
Solyc03g120380.3	1.30301	<i>Auxin-regulated IAA19</i>	<i>IAA19</i>	AT3G15540	<i>IAA19</i>
Solyc04g082830.3	-1.85963	<i>Auxin efflux carrier family protein</i>	<i>Solyc04g082830</i>	AT1G20925	<i>PIN-likes1</i>
Solyc02g037550.3	-1.54635	<i>Auxin efflux carrier family protein</i>	<i>Solyc02g037550</i>	AT1G76520	<i>PIN-likes3</i>
Solyc03g031990.3	-0.89102	<i>Auxin efflux carrier family protein</i>	<i>Solyc03g031990</i>	AT1G76520	<i>PIN-likes3</i>
Solyc02g091240.1	-0.76972	<i>Auxin efflux carrier family protein</i>	<i>Solyc02g091240</i>	AT1G71090	<i>PIN-likes2</i>
Solyc11g069500.2	-0.71450	<i>Auxin response factor 10A</i>	<i>ARF10A</i>	AT2G28350	<i>ARF10</i>
Solyc06g075360.3	1.14777	<i>Tetraspanin-3-like</i>	<i>Solyc06g075360</i>	AT3G45600	<i>TET3</i>
Solyc12g007230.2	-0.77621	<i>Auxin-regulated IAA8</i>	<i>IAA8</i>	AT4G29080	<i>IAA27</i>
Solyc08g082630.3	-1.12841	<i>Auxin response factor 9A</i>	<i>ARF9A</i>	AT4G23980	<i>ARF9</i>
Solyc07g025510.3	-0.74116	<i>Senescence-associated protein</i>	<i>Solyc07g025510</i>	AT2G19580	<i>TET2</i>

Solyc06g053840.3	-0,74270	<i>Auxin-regulated IAA4</i>	<i>IAA4</i>	AT5G43700	<i>IAA4</i>
Solyc08g080730.3	-0.94883	<i>Tetraspanin-10</i>	<i>Solyc08g080730</i>	AT1G56700	<i>TET10</i>
Solyc03g116100.3	-2.08677	<i>R2R3MYB transcription factor 31</i>	<i>MYB31</i>	AT5g62470	<i>MYB5</i>
Solyc07g014620.1	-2.55421	<i>Small auxin up-regulated RNA63</i>	<i>SAUR63</i>	AT5G20810	<i>SAUR70</i>
Solyc06g053260.1	-1.29932	<i>Small auxin up-regulated RNA 58</i>	<i>SAUR58</i>	AT4G00880	<i>SAUR31</i>
Solyc02g067340.3	1.44044	<i>R2R3MYB transcription factor 96</i>	<i>THM6</i>	AT3G47600	<i>MYB94</i>
Solyc01g110680.3	-1.33216	<i>Small auxin up-regulated RNA12</i>	<i>SAUR12</i>	AT2G21210	<i>SAUR6</i>
Solyc02g087960.3	2.57066	<i>R2R3MYB transcription factor 94</i>	<i>MYB94</i>	AT3G47600	<i>MYB94</i>
Solyc11g011660.2	1.46882	<i>Auxin-induced SAUR</i>	<i>Solyc11g011660</i>	AT1G29500	<i>SAUR66</i>
Solyc10g083320.2	3.74462	<i>Small auxin up-regulated RNA82</i>	<i>SAUR82</i>	AT2G36210	<i>SAUR45</i>
Solyc01g111000.3	-1.42006	<i>Auxin-induced SAUR-like</i>	<i>Solyc01g111000</i>	AT4G38840	<i>SAUR14</i>
Solyc01g096340.3	-0.72682	<i>Small auxin up-regulated RNA2</i>	<i>SAUR2</i>	AT3G61900	<i>SAUR33</i>
Solyc04g052970.2	1.98848	<i>Auxin-induced SAUR-like</i>	<i>Solyc04g052970</i>	AT5G18030	<i>SAUR21</i>
Solyc01g110560.3	-1.02335	<i>Small auxin up-regulated RNA3</i>	<i>SAUR3</i>	AT4G34750	<i>SAUR49</i>
Solyc01g110940.3	1.27774	<i>Auxin-induced SAUR-like</i>	<i>Solyc01g110940</i>	AT4G38840	<i>SAUR14</i>
Solyc01g110590.3	1.23355	<i>Small auxin up-regulated RNA6</i>	<i>SAUR6</i>	AT4G34760	<i>SAUR50</i>
Solyc04g078900.3	0.95678	<i>Abscisic acid 8'-hydroxylase CYP707A1</i>	<i>CYP707A1</i>	AT3G19270	<i>CYP707A4</i>
Solyc04g053000.1	1.33901	<i>Auxin-induced SAUR-like</i>	<i>Solyc04g053000</i>	AT5G18030	<i>SAUR21</i>
Solyc06g053290.1	-0.73484	<i>Small auxin up-regulated RNA59</i>	<i>SAUR59</i>	AT2G46690	<i>SAUR32</i>

353
354
355

Table S3. Tomato DEGs involved in gibberellin signalling (included in the KEGG ID: sly04075) and biosynthesis (included in the KEGG ID: sly01110) as retrieved from KEGG maps after the enrichment analysis.

Gene ID	log ₂ FC	ITAG 3.0 annotation	<i>S. lycopersicum</i> gene acronym	<i>A. thaliana</i> orthologue	<i>A. thaliana</i> gene acronym
GA signalling					
Solyc04g078390.2	-0.72	<i>F-box family protein</i>	<i>SLY1</i>	AT4G24210	<i>SLY1 (GID2)</i>
Solyc01g098390.3	-1.52	<i>Gibberellin receptor GID1A</i>	<i>GID1a</i>	AT5G27320	<i>GID1C</i>
Solyc09g074270.3	-1.57	<i>Gid1-like gibberellin receptor</i>	<i>GID1b1</i>	AT3G63010	<i>GID1B</i>
Solyc01g102300.3	-2.81	<i>bHLH transcription factor 006</i>	<i>PIF3</i>	AT1G09530	<i>PIF3</i>
GA metabolism					
Solyc03g119910.3	3.64	<i>Le3OH-23b-hydroxylase</i>	<i>GA3ox-2</i>	AT1G15550	<i>GA3OX1</i>
Solyc06g035530.3	2.70	<i>Gibberellin 20-oxidase-2</i>	<i>GA20ox-2</i>	AT4G25420	<i>GA20OX1</i>
Solyc07g056670.3	2.60	<i>Gibberellin 2-oxidase 2</i>	<i>GA2ox-2</i>	AT1G78440	<i>GA2OX1</i>
Solyc01g079200.3	2.29	<i>Gibberellin 2-oxidase 3</i>	<i>GA2ox-3</i>	AT1G02400	<i>GA2OX6</i>
Solyc07g066675.1	-1.30	<i>Ent-kaurene synthase</i>	<i>TPS24 (KS)</i>	AT1G79460	<i>GA2</i>
Solyc07g066670.3	-1.62	<i>Ent-kaurene synthase</i>	<i>TPS24 (KS)</i>	AT1G79460	<i>GA2</i>
Solyc07g061720.3	-2.12	<i>Gibberellin 2-oxidase-4</i>	<i>GA2ox-4</i>	AT1G78440	<i>GA2OX1</i>
Solyc04g083160.2	-2.44	<i>Cytochrome P450</i>	<i>KO</i>	AT5G25900	<i>KO</i>
Solyc06g084240.2	-4.09	<i>Copalyl diphosphate synthase</i>	<i>TPS40 (CPS)</i>	AT4G02780	<i>GA1</i>

356
357

358 **Table S4.** Expressed genes passing quality checks, trimming and FPKM filtering in 3
 359 independent replicates of wild-type *Solanum lycopersicum* M82 (wt) or CCD7-silenced leaves
 360 in the same background (SL-). SL 3.0: *Solanum lycopersicum* (tomato) genome assembly
 361 SL3.0 from the Solanaceae Genomics Project.

Sample	No. of clean reads x 10 ⁶	Aligned reads on SL 3.0 (%)	No. of expressed transcripts
wt_1	47.29	85.45	18791
wt_2	42.92	84.64	18615
wt_3	31.63	85.40	19048
SL-_1	32.06	85.25	18702
SL-_2	36.99	86.75	18261
SL-_3	39.09	86.96	18626

362
 363
 364

365 **Table S5.** List of primers used in this work, with target gene names.

primer/ target	sequence	reference
<i>ACT</i>	5'-TCCCAGGTATTGCTGATAGAA-3' 5'-TGAGGGAAGCCAAGATAGAG -3'	(43)
<i>AN</i>	5'-CCATAATCCCCTGCCTCCA-3' 5'-TCCCCTGTACATGCACCATT-3'	This work
<i>AP1/MC</i>	5'-CGAGAAAGAACCAACTCATGC-3' 5'-TAGTTTGCTGGTGCCATTCA-3'	(44)
<i>ARF5</i>	5'-ATTAGTTCTGAGTTGTGGC-3' 5'-GGTATCTGTGAAGTTGCTG-3'	(45)
<i>DOF9</i>	5'-ATGGTGCTGGAGCGAGTATG-3' 5'-GCGTAGAAATAGCAAGATCTGGGA-3'	This work
<i>DST</i>	5'-TTTGCCTGTGGAGAGGAGAGGAAA-3' 5'-ACTCAACGCGCAGAACGTAACGAT-3'	This work
<i>EF-1α</i>	5'-CTCCATTGGGTCTG TTTTGCT-3' 5'-GGTCACCTTGGC ACCAGTTG-3'	(46)
<i>FA</i>	5'-AGGGGAAGAGGATGAGGAAA-3' 5'-GATGCTCCCTTTGTCTCTCG-3'	(44)
<i>FUL1</i>	5'-GTTTTGCCACAACAACCTGGACTC-3' 5'-CTTGCTGCTGTGAAGAACTACC-3'	(47)
<i>GA20ox2</i>	5'-TTTCCATATTCTACCCTACAAG -3' 5'-TCATCGCATTACAATACTCTT -3'	(48)
<i>GA2ox4</i>	5'-CCAACAACACTTCCGGTCTT-3' 5'-CATTCGTCATCACCTGTAATGAG-3'	(49)
<i>GA3ox2</i>	5'-GATCATAAATTTGTCATGGATAC -3' 5'-TGTTTCCATATGGTTAAGTAATCG -3'	(50)
<i>LA</i>	5'-TGCAGCAGCTATTCGGTCAA-3' 5'-ACCCAGAGAATCCGCCTACT-3'	(51)
<i>LIN</i>	5'-AGTGCCAAACAGGTACAATGTG-3' 5'-CCATTCAAAGCATCCATCCTGG-3'	This work
<i>MBP20</i>	5'-CACATTCTCACCACCAACTTCCTAA-3' 5'-AGTGATGAGCCTGACCGGAT-3'	(1)
<i>SBP3</i>	5'-CAAGTTGAACGGGCACCTAC-3' 5'-TGGCAAATGACAGAAGAGAGAG-3'	(44)
<i>SBP15</i>	5'-GGTTCAGCTACCAGGACCAG-3' 5'-TGTGAACTTGGCTGTTGACC-3'	(44)
<i>SFT</i>	5'-GTCACCGATATTCCAGCTACC-3' 5'-CATACACTGTTTGCCGACCTA-3'	This work
<i>snRU6</i>	5'-GGGAACGATACAGAGAAGATTAGC-3' 5'-ACCATTCTCGATTTGTGCGT-3'	(52)
<i>SP5G</i>	5'-CTAGCAACCCAAACCTGAGG-3' 5'-ATTGCCAAAGGTTGCTCCTG-3'	This work

<i>SP6A</i>	5'-TGGTCGTGTGATAGGTGAAGT-3' 5'-CTGTGACCAGCCAGTGTAGA-3'	This work
<i>TR5</i>	5'-GCAGCGATCACAGAGGAATC-3' 5-TGGCTTCCTTCCATCAACCT-3'	This work
<i>UF</i>	5'-CCCCGGTGGTTCTAAAATGG-3' 5'-TCAACTTGTTGAAAGGCATCGT-3'	This work
<i>WOX9</i>	5'-TGCAGTCACAGCTCATGAGT-3' 5'-TCCCAACCTCAAAAGCAACG-3'	This work
Stem-loop miR156	5'- GTCGTATCCAGTGCAGGGTCCGAGGTAT TCGCACTGGATACGACGTGCTC-3'	(53)
Mature miR156	5'-GTCGTATCCAGTGCAGGGT-3' 5'-TTGACAGAAGATAGAGAGCACG-3'	(52)
Stem-loop miR319	5'- GTCGTATCCAGTGCAGGGTCCGAGGTAT TCGCACTGGATACGAGGGAGC-3'	(54)
Mature miR319	5'-GCGGCGTTGGACTGAAGGGT-3' 5'-GTGCAGGGTCCGAGG-3'	(54)

366
367

368
369
370
371
372
373
374
375
376

Dataset S1 (separate file). Gene ontology categories for Biological Processes (BP-GO) enriched in strigolactone-depleted (SL-) tomato leaves in comparison to wt (FDR<0.05; log₂FC >+0.7;<-0.7), obtained using the ShinyGO v0.61 Gene Ontology Enrichment Analysis tool.

Dataset S2 (separate file). List of DEGs included in the GO category Reproduction (GO: 0000003).

Dataset S3 (separate file). List of differentially expressed genes (DEGs) in the strigolactone-depleted (SL-) plants with respect to wt (padjust ≤ 0.05).

377
378
379

SI References

- 380 1. X. Jiang *et al.*, *FRUITFULL-like* genes regulate flowering time and inflorescence
381 architecture in tomato. *Plant Cell* **34**, 1002-1019 (2022).
- 382 2. R. Wang *et al.*, Re-evaluation of transcription factor function in tomato fruit
383 development and ripening with CRISPR/Cas9-mutagenesis. *Sci. Rep.* **9**, 1696 (2019).
- 384 3. C. Périlleux, G. Lobet, P. Tocquin, Inflorescence development in tomato: gene
385 functions within a zigzag model. *Front. Plant Sci.* **5**, 121 (2014).
- 386 4. E. Gimenez *et al.*, *TOMATO AGAMOUS1* and *ARLEQUIN/TOMATO AGAMOUS-LIKE1*
387 *MADS*-box genes have redundant and divergent functions required for tomato
388 reproductive development. *Plant Mol. Biol.* **91**, 513-531 (2016).
- 389 5. T. Yang, Y. He, S. Niu, S. Yan, Y. Zhang, Identification and characterization of the
390 *CONSTANS (CO)/CONSTANS-like (COL)* genes related to photoperiodic signaling and
391 flowering in tomato. *Plant Sci.* **301**, 110653 (2020).
- 392 6. X. Ma *et al.*, The NAC transcription factor *SINAP2* regulates leaf senescence and fruit
393 yield in tomato. *Plant Physiol.* **177**, 1286-1302 (2018).
- 394 7. Y. Berger *et al.*, The NAC-domain transcription factor *GOBLET* specifies leaflet
395 boundaries in compound tomato leaves. *Development* **136**, 823-832 (2009).
- 396 8. A. Hendelman, R. Stav, H. Zemach, T. Arazi, The tomato NAC transcription factor
397 *SINAM2* is involved in flower-boundary morphogenesis. *J. Exp. Bot.* **64**, 5497-5507
398 (2013).
- 399 9. C. Bendix, C. M. Marshall, F. G. Harmon, Circadian clock genes universally control key
400 agricultural traits. *Mol. Plant* **8**, 1135-1152 (2015).
- 401 10. P. Facella *et al.*, Diurnal and circadian rhythms in the tomato transcriptome and their
402 modulation by cryptochrome photoreceptors. *PLoS One* **3**, e2798 (2008).
- 403 11. Y. Tanigaki *et al.*, Transcriptome analysis of plant hormone-related tomato (*Solanum*
404 *lycopersicum*) genes in a sunlight-type plant factory. *PLoS One* **10**, e0143412 (2015).
- 405 12. R. Schaffer *et al.*, The late elongated hypocotyl mutation of *Arabidopsis* disrupts
406 circadian rhythms and the photoperiodic control of flowering. *Cell* **93**, 1219-1229
407 (1998).
- 408 13. J. L. Prunedo-Paz, G. Breton, A. Para, S. A. Kay, A functional genomics approach
409 reveals CHE as a component of the *Arabidopsis* circadian clock. *Science* **323**, 1481-
410 1485 (2009).
- 411 14. X. W. Deng, T. Caspar, P. H. Quail, *COP1*: a regulatory locus involved in light-
412 controlled development and gene expression in *Arabidopsis*. *Genes Dev.* **5**, 1172-
413 1182 (1991).
- 414 15. S. Jang *et al.*, *Arabidopsis COP1* shapes the temporal pattern of CO accumulation
415 conferring a photoperiodic flowering response. *EMBO J.* **27**, 1277-1288 (2008).
- 416 16. M. R. Doyle *et al.*, The *ELF4* gene controls circadian rhythms and flowering time in
417 *Arabidopsis thaliana*. *Nature* **419**, 74-77 (2002).

- 418 17. J. W. Yu *et al.*, COP1 and ELF3 control circadian function and photoperiodic flowering
419 by regulating GI stability. *Mol. Cell* **32**, 617-630 (2008).
- 420 18. Y. He, M. R. Doyle, R. M. Amasino, PAF1-complex-mediated histone methylation of
421 *FLOWERING LOCUS C* chromatin is required for the vernalization-responsive, winter-
422 annual habit in Arabidopsis. *Genes Dev.* **18**, 2774-2784 (2004).
- 423 19. C. Brandoli, C. Petri, M. Egea-Cortines, J. Weiss, Gigantea: uncovering new functions
424 in flower development. *Genes* **11** (2020).
- 425 20. M. Y. Chung *et al.*, Ectopic expression of miRNA172 in tomato (*Solanum*
426 *lycopersicum*) reveals novel function in fruit development through regulation of an
427 AP2 transcription factor. *BMC Plant Biol.* **20**, 283 (2020).
- 428 21. X. Liu *et al.*, The NF-YC-RGL2 module integrates GA and ABA signalling to regulate
429 seed germination in Arabidopsis. *Nat. Comm.* **7**, 12768 (2016).
- 430 22. B. B. Aklilu, R. S. Soderquist, K. M. Culligan, Genetic analysis of the Replication
431 Protein A large subunit family in Arabidopsis reveals unique and overlapping roles in
432 DNA repair, meiosis and DNA replication. *Nucleic Acids Res.* **42**, 3104-3118 (2014).
- 433 23. Y. Steinbach, L. Hennig, Arabidopsis MSI1 functions in photoperiodic flowering time
434 control. *Front. Plant Sci.* **5**, 77 (2014).
- 435 24. Y. Z. Xu *et al.*, The chloroplast triggers developmental reprogramming when *MutS*
436 *HOMOLOG1* is suppressed in plants. *Plant Physiol.* **159**, 710-720 (2012).
- 437 25. S. Sarma *et al.*, *MutS-Homolog2* silencing generates tetraploid meiocytes in tomato.
438 *Plant Direct* **2**, e00017 (2018).
- 439 26. H. Saze, T. Kakutani, Heritable epigenetic mutation of a transposon-flanked
440 Arabidopsis gene due to lack of the chromatin-remodeling factor DDM1. *EMBO J.* **26**,
441 3641-3652 (2007).
- 442 27. C. Cosio *et al.*, The class III peroxidase PRX17 is a direct target of the MADS-box
443 transcription factor AGAMOUS-LIKE15 (AGL15) and participates in lignified tissue
444 formation. *New Phytol.* **213**, 250-263 (2017).
- 445 28. J. T. Vogel *et al.*, *SICCD7* controls strigolactone biosynthesis, shoot branching and
446 mycorrhiza-induced apocarotenoid formation in tomato. *Plant J.* **61**, 300-311 (2010).
- 447 29. Y. Burko *et al.*, A role for APETALA1/fruitfull transcription factors in tomato leaf
448 development. *Plant Cell* **25**, 2070-2083 (2013).
- 449 30. N. Ori *et al.*, Regulation of *LANCEOLATE* by miR319 is required for compound-leaf
450 development in tomato. *Nat. Genet.* **39**, 787-791 (2007).
- 451 31. P. Pesaresi, C. Mizzotti, M. Colombo, M. Masiero, Genetic regulation and structural
452 changes during tomato fruit development and ripening. *Front. Plant Sci.* **5**, 124
453 (2014).
- 454 32. A. Mazzucato, A. Taddei, G. Soressi, The parthenocarpic fruit (*pat*) mutant of tomato
455 (*Lycopersicon esculentum* Mill.) sets seedless fruits and has aberrant anther and
456 ovule development. *Development* **125**, 107-114 (1998).
- 457 33. M. Pertea, D. Kim, G. M. Pertea, J. T. Leek, S. L. Salzberg, Transcript-level expression
458 analysis of RNA-seq experiments with HISAT, StringTie and Ballgown. *Nat. Protoc.*
459 **11**, 1650-1667 (2016).
- 460 34. S. Anders, P. T. Pyl, W. Huber, HTSeq--a Python framework to work with high-
461 throughput sequencing data. *Bioinformatics* **31**, 166-169 (2015).
- 462 35. M. I. Love, W. Huber, S. Anders, Moderated estimation of fold change and dispersion
463 for RNA-seq data with DESeq2. *Genome Biol.* **15**, 550 (2014).
- 464 36. M. Kanehisa, Enzyme annotation and metabolic reconstruction using KEGG.
465 *Methods Mol. Biol.* **1611**, 135-145 (2017).
- 466 37. S. X. Ge, D. Jung, R. Yao, ShinyGO: a graphical gene-set enrichment tool for animals
467 and plants. *Bioinformatics* **36**, 2628-2629 (2020).

- 468 38. T. Urbanová, D. Tarkowská, O. Novák, P. Hedden, M. Strnad, Analysis of gibberellins
469 as free acids by ultra performance liquid chromatography-tandem mass
470 spectrometry. *Talanta* **112**, 85-94 (2013).
- 471 39. D. Rittenberg, G. L. Foster, A new procedure for quantitative analysis by isotope
472 dilution, with application to the determination of amino acids and fatty acids. *J. Biol.*
473 *Chem.* **133**, 737-744 (1940).
- 474 40. C. Pagliarani *et al.*, The accumulation of miRNAs differentially modulated by drought
475 stress is affected by grafting in grapevine. *Plant Physiol.* **173**, 2180-2195 (2017).
- 476 41. C. Everaert *et al.*, Benchmarking of RNA-sequencing analysis workflows using whole-
477 transcriptome RT-qPCR expression data. *Sci. Rep.* **7**, 1559 (2017).
- 478 42. J. H. Zar, Spearman Rank Correlation: Overview. *Wiley StatsRef: Statistics Reference*
479 *Online* <https://doi.org/10.1002/9781118445112.stat05964> (2014).
- 480 43. J. López-Ráez *et al.*, Does abscisic acid affect strigolactone biosynthesis? *New Phytol.*
481 **187**, 343-354 (2010).
- 482 44. G. F. Ferreira e Silva *et al.*, MicroRNA156-targeted SPL/SBP box transcription factors
483 regulate tomato ovary and fruit development. *Plant J.* **78**, 604-618 (2014).
- 484 45. S. Habib, M. Waseem, N. Li, L. Yang, Z. Li, Overexpression of *SlGRAS7* affects multiple
485 behaviors leading to confer abiotic stresses tolerance and impacts gibberellin and
486 auxin signaling in tomato. *Int. J. Genomics* **2019**, 4051981 (2019).
- 487 46. M. Digilio *et al.*, Molecular and chemical mechanisms involved in aphid resistance in
488 cultivated tomato. *New Phytol.* **187**, 1089-1101 (2010).
- 489 47. M. Bemer *et al.*, The tomato FRUITFULL homologs TDR4/FUL1 and MBP7/FUL2
490 regulate ethylene-independent aspects of fruit ripening. *Plant Cell* **24**, 4437-4451
491 (2012).
- 492 48. Y. Chen *et al.*, Overexpression of bHLH95, a basic helix-loop-helix transcription
493 factor family member, impacts trichome formation via regulating gibberellin
494 biosynthesis in tomato *J. Exp. Bot.* **71**, 3450-3462 (2020).
- 495 49. O. Yanai, E. Shani, D. Russ, N. Ori, Gibberellin partly mediates LANCEOLATE activity in
496 tomato. *Plant J.* **68**, 571-582 (2011).
- 497 50. S. Matsuo, K. Nanya, S. Imanishi, I. Honda, E. Goto, Effects of blue and red lights on
498 gibberellin metabolism in tomato seedlings. *Hort. J.* **88**, 76-82 (2019).
- 499 51. G. F. F. Silva *et al.*, Tomato floral induction and flower development are orchestrated
500 by the interplay between gibberellin and two unrelated microRNA-controlled
501 modules. *New Phytol.* **221**, 1328-1344 (2019).
- 502 52. I. Visentin *et al.*, A novel strigolactone-miR156 module controls stomatal behaviour
503 during drought recovery. *Plant Cell Environ.* **43**, 1613-1624 (2020).
- 504 53. C. Chen *et al.*, Real-time quantification of microRNAs by stem-loop RT-PCR *Nucleic*
505 *Acids Res.* **33**, e179 (2005).
- 506 54. A. Zanca *et al.*, Identification and expression analysis of microRNAs and targets in
507 the biofuel crop sugarcane. *BMC Plant Biol.* **10**, 260 (2010).